Journal of Statistical Mechanics:
Theory and Experiment

PAPER: CLASSICAL STATISTICAL MECHANICS, EQUILIBRIUM AND NON-EQUILIBRIUM

Theoretical study of network junction models for totally asymmetric exclusion processes with interacting particles

Journal of Statistical Mechanics: Theory and Experiment
An IOP and SISSA journal

PAPER: Classical statistical mechanics, equilibrium and non-equilibrium

Theoretical study of network junction models for totally asymmetric exclusion processes with interacting particles

Tripti Midha[1], Anatoly B Kolomeisky[2] and Arvind Kumar Gupta[1]

[1] Department of Mathematics, Indian Institute of Technology Ropar, Rupnagar-140001, Punjab, India
[2] Department of Chemistry and Chemical and Biomolecular Engineering, Rice University, Houston, TX 77005, United States of America
E-mail: akgupta@iitrpr.ac.in

Received 2 May 2019
Accepted for publication 31 May 2019
Published 6 August 2019

Online at stacks.iop.org/JSTAT/2019/083202
https://doi.org/10.1088/1742-5468/ab310d

Abstract. Biological transport phenomena frequently exhibit complex network behavior when several molecular fluxes converge to special junctions from which another fluxes move out in different directions. Similar behavior is also observed in vehicular transport. Stimulated by these observations, we developed a theoretical framework to investigate network junction models of totally asymmetric simple exclusion processes with interacting particles. Utilizing a two-site cluster mean field framework that takes into account some correlations in the system, stationary dynamic properties, such as phase diagrams, density profiles and correlations profiles, are explicitly evaluated. It is found that the number of stationary phases strongly depend on the number of segments that come and leave the network junction. The inter-particle interactions also have a strong effect of dynamic properties of the system. Our method can be extended to the systems with several junctions. All theoretical predictions are in good agreement with extensive Monte Carlo computer simulations.

Keywords: driven diffusive systems, exclusion processes, molecular motors, network dynamics

1742-5468/19/083202+19$33.00

Contents

1. Introduction

Non-equilibrium transport models have gained much popularity from the theoretical as well as applications point of view [1–3]. One such non-equilibrium driven model is totally asymmetric simple exclusion process (TASEP), in which particles hop forward along a one-dimensional lattice with a unit rate [4, 5]. They interact only under the hard-core exclusion principle, which guarantees no more than a single particle at a lattice site. Over the years, TASEP has captured the position of a paradigmatic model among the class of driven diffusive lattice models. It has been thoroughly explored under various boundary conditions and via several theories [6, 7] and in particular, for the open boundary conditions, it displays several interesting phenomena such as boundary-induced phase transitions, spontaneous-symmetry breaking, etc [3, 8, 9]. Several generalizations of TASEP have provided their contribution to understand the mechanisms of biological and vehicular transport processes such as traffic flow, intracellular transport, surface growth, transport in ion channels, mRNA translation, etc [10–16].

The one-dimensional (1D) TASEP with nearest-neighbor interactions is one of the variants of simple TASEP that has gained much attention for its relevancy in the dynamics of motor proteins and vehicular transport [17–21]. The KLS is a primarily model for the interactions, in which the hopping rates of the particles depend on the four following sites and that displays exciting features such as downward shocks [22]. Some recent research on motor proteins reveal that their dynamics on the microtubules is affected in the presence of interaction energy [23, 24]. This has motivated to incorporate the nearest-neighbor interactions among the particles in a thermodynamic

J. Stat. Mech. (2019) 083202

consistent way, which is relevant to biological motor proteins as well as to other transport processes. The TASEP model with thermodynamically consistent interactions has been analyzed using different approximate theories, such as cluster mean-field [20], two-cluster mean-field theory [21], and modified cluster mean-field theory [25].

One of the major challenges in the application of TASEP and its many variants to the real world situations is the inter-connectivity of a manifold of segments. In biological transport processes, experiments indicate the presence of junctions and the lattice defects. For instance, in protein secretion, there are storage structures for proteins, which may be called as junctions, at which a large number of individual microtubules meet and the coupling of segment-wise transport arises. The junctions also play a crucial role in vehicular transport processes for they constitute bottlenecks for the flow of particles. Blockages have been seen to arise, depending on the overall density of particles. They induce a traffic-jam-like back-lag of particles, and therefore affect the transport far beyond a local scale. In this regard, many theoretical models and studies revealing the dynamics of networks of several simple TASEP segments have been performed [26–31]. In particular, in [27], the topological coupling of simple TASEP segments is achieved by introducing an explicit junction site, at which all four TASEP segments meet. The phase behavior of the composed system was deduced by matching the well known TASEP phases of the individual segments, subject to current conservation at the junctions. They proposed the explicit-vertex procedure, which was successful in analyzing the stationary phases of TASEP-like transport through complex networks in a mean-field approximation [32–35]. Also in [26], the simple mean-field approach was utilized to analyze a network made up of coupling of two parallel simple TASEP segments with an individual segment. However, the literature on networks is still deprived of the study of networks of interacting TASEP segments.

In this work, we consider a junction vertex v at which m similar TASEP segments with mutual interactions enter. From the vertex, n identical TASEP segments with interactions leave. Such vertex is labeled as $V(m:n)$, i.e. a vertex with m incoming segments and n outgoing segments. The paper is organized as follows. In section 2, we briefly discuss the results for a single channel interacting TASEP model. In section 3, we provide the description of the model and the theoretical approach. The phase diagrams are theoretically computed in section 4, and is followed by the results and discussions in section 5. Finally, we summarize and conclude in section 6.

2. Brief discussion on single-channel open interacting TASEP model

In this section, we discuss the bulk and the boundary properties of single channel interacting TASEP model, where interactions are incorporated in a thermodynamic consistent way. In the interacting TASEP model, it is assumed that any two nearest neighboring particles form a bond with energy E. The rate of hopping of particles, which leads to the formation or destruction of these bonds, depends upon E. If the particle hopping leads to the bond formation (destruction), the hopping rate is $q = \mathrm{e}^{\theta E}$ ($r = \mathrm{e}^{(\theta-1)E}$). Otherwise, when bond formation and destruction occur simultaneously or neither of them occur, the hopping rate is 1 (see figure 1). Here, E is expressed in units

J. Stat. Mech. (2019) 083202

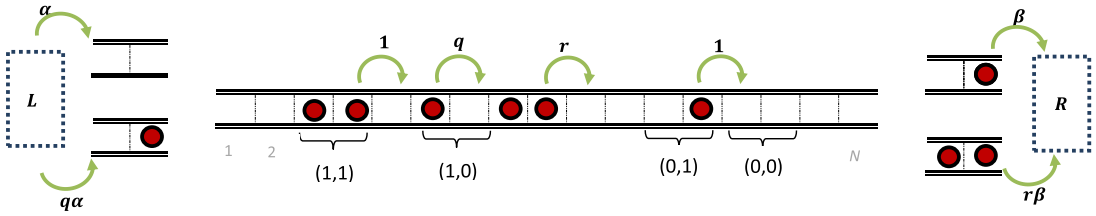

Figure 1. Schematic view of a single channel open interacting TASEP model. Filled circles represent particles, while empty sites indicate absence of particles. L and R are, rescpectively, left and right, reservoirs.

of $k_{\mathrm{B}}T$ and the the rates q and r follow the relation $\frac{q}{r} = \mathrm{e}^{E}$ [20] due to the interpretation of the phenomenon of creating and breaking of bonds between pair of particles as reversible chemical reaction. The parameter θ $(0 \leqslant \theta \leqslant 1)$ is a dimensionless splitting parameter that quantifies how much the transitions rates are affected by the interaction energy. The interactions are attractive (repulsive) for $E > 0$ $(E < 0)$. Clearly, for the case of attractive interactions, we obtain $q > 1$ and $r < 1$, while the repulsive interactions make $r > 1$ and $q < 1$. Figure 1 shows the schematic view of an open single channel interacting TASEP model consisting of total N lattice sites. We can see from the figure that the bond formation and bond destruction affect the entrance rate α and exit rate β, respectively. A particle enters from an infinite left reservoir L with a rate α when both the first as well as second sites of the lattice are empty. Whereas, the rate of entrance is modified to $q\alpha$ when the first and the second sites are empty and occupied, respectively. The rate of exit of a particle present at the Nth site into an infinite right reservoir R is β when the $N-1$th site is empty; otherwise the rate is $r\beta$ due to bond breaking. For the case of zero energy, the rates, the model reduces to the simple TASEP with rates $q = r = 1$.

The bulk properties of the interacting TASEP model under both open and periodic boundary conditions has been well examined in the literature, using the two-cluster mean-field theory [21]. In the two-cluster mean-field approach, the probability of clusters of size three or more are written as the product of clusters of size two, for details refer [21]. The four possible two-clusters in a lattice, where '1'('0'), represents the occupied (empty) site are shown in figure 1. We write the particle current in terms of the average particle density, ρ, and the two-cluster probability P_{10} for two-cluster $(1,0)$ as follows.

$$J = \frac{P_{10}[P_{10} + (q-2)P_{10}^2 + r(\rho - P_{10})(1-\rho-P_{10})]}{\rho(1-\rho)}, \tag{1}$$

where $P_{10} = \frac{-r+\sqrt{r^2+4(q-r)r\rho(1-\rho)}}{2(q-r)}$. Substituting P_{10} in equation (1), one can obtain the particle current, explicitly as a function of particle density ρ. For the thermodynamically consistent boundary conditions, the single-channel interacting TASEP model has three phases namely low-density (LD), high-density (HD) and maximal current (MC). We denote the homogeneous bulk particle density for site i $(2 \leqslant i \leqslant N-1)$ in a phase $\in$ {LD,HD,MC} by ρ_{Phase} (given in table 1). Correspondingly, the particle current in that phase is denoted by J_{Phase} and can be obtained by substituting the densities of the respective phases in the current expression given by equation (1). The density ρ_{LD} in

Table 1. Mean-field expressions of the bulk and the boundary densities for the single channel interacting TASEP segment with left and right reservoir density as α and β,respectively and for $E > -2.885k_{\rm B}T$, $\theta = 0.5$.

Phase	$\rho_{\rm bulk}$	ρ_1	ρ_L
LD	$\rho_{\rm LD} = \frac{1}{2}\left(1 + \frac{\alpha(q+1)-1-(\alpha q(q+1)-1)\sqrt{(1+\alpha(q-1)^2(\alpha(q+1)^2-2))}}{2+\alpha(q^2-1)(\alpha q(q+1)-2)}\right)$	$\rho_{\rm LD}$	$\frac{J_{\rm LD}}{\beta(1+(r-1)\rho_{\rm LD})}$
HD	$\rho_{\rm HD} = \frac{1}{2}\left(1 + \frac{(q-\beta(q+1)+(\beta(q+1)-1)\sqrt{\beta^2(q^2-1)^2-2\beta q(q-1)^2+q^2}}{2q+\beta(q^2-1)(\beta(q+1)-2)}\right)$	$1 - \frac{J_{\rm HD}}{\alpha(1+(q-1)\rho_{\rm HD})}$	$\rho_{\rm HD}$
MC	$\rho_{\rm MC} = 0.5$	$1 - \frac{J_{\rm MC}}{\alpha(1+(q-1)\rho_{\rm MC})}$	$\frac{J_{\rm MC}}{\beta(1+(r-1)\rho_{\rm MC})}$.

the LD phase is obtained by equating the entrance current, $J_{\rm LD} = \alpha(P_{00} + qP_{01})$, with the bulk current given by equation (1) and solving for $\rho_{\rm bulk} = \rho_{\rm LD}$. Similarly, the solution ρ obtained by equating the exit current, $J_{\rm HD} = \beta(P_{01} + rP_{11})$, with the bulk current from equation (1) yields the density $\rho = \rho_{\rm HD}$ in the HD phase. Here, P_{00}, P_{11} and P_{01}, respectively denote the probabilities of the two-clusters $(0,0)$, $(1,1)$ and $(0,1)$, as shown in figure 1. For the two-cmf theory, the particle-hole symmetry in the bulk yields $P_{10} = P_{01}$. Further, the Kolmogorov Consistency conditions for the particle density ρ in the bulk implies $P_{00} = 1 - \rho - P_{10}$ and $P_{11} = \rho - P_{10}$. The bulk particle density in the MC phase is obtained by solving $\partial J/\partial\rho = 0$ for the maximal density $\rho = \rho_{\rm MC}$. The existence conditions for the phases are described below.

$$\text{LD} \quad \text{if} \quad \alpha < \frac{\beta}{\sqrt{q/r}}, \quad \alpha < \alpha_c,$$

$$\text{HD} \quad \text{if} \quad \alpha > \frac{\beta}{\sqrt{q/r}}, \quad \beta < \beta_c,$$

$$\text{MC} \quad \text{if} \quad \alpha \geqslant \alpha_c, \quad \beta \geqslant \beta_c,$$

where α_c and β_c are the triple points separating the three phases. The first-order continuous phase transition line $\alpha = \sqrt{\frac{r}{q}}\beta$, separating the LD and HD phases is obtained by the current continuity condition for $J_{\rm LD}$ and $J_{\rm HD}$. While the triple points and correspondingly the phase transition lines separating the LD and the HD phases from the MC phase are, respectively, obtained by equating the current $J_{\rm LD}$ and $J_{\rm HD}$ with $J_{\rm MC}$ and tending the $\rho_{\rm LD}$ and $\rho_{\rm HD}$ to $\rho_{\rm MC}$. It has been found in [21] that for $E > E_c(\theta)$, $\rho_{\rm MC} = 0.5$, independent of energy E. In particular, for $\theta = 0$, $E_c(0) \approx -4.87k_{\rm B}T$, while for $\theta = 0.5$, $E_c(0.5) \approx -2.885k_{\rm B}T$ and $\theta = 1$ yields $E_c(1) \approx -1.76k_{\rm B}T$, as computed in [21]. Figure 2 shows the triple points with respect to interaction energy E, when $\rho_{\rm MC} = 0.5$ for any value of splitting parameter θ. In this case, $\alpha_c = \frac{r[q^2(6r-2(1+\sqrt{qr}))+q(6\sqrt{qr}+r(2r-6(1+\sqrt{qr})))+2r\sqrt{qr}]}{(q-r)^2(\sqrt{qr}+q(r-(1+\sqrt{qr})))}$ and $\beta_c = \sqrt{q/r}\ \alpha_c$. One of the key findings from figure 2 is that the triple points remain invariant with respect to the splitting parameter θ, under the proposed transition rules in the model. Therefore, for the simplicity in obtaining the results for the networks, we choose $\theta = 0.5$, that also splits the interaction energy with maximum effect on both the rates q and r, simultaneously. Further, for any energy $E > -2.885k_{\rm B}T$, the maximal

J. Stat. Mech. (2019) 083202

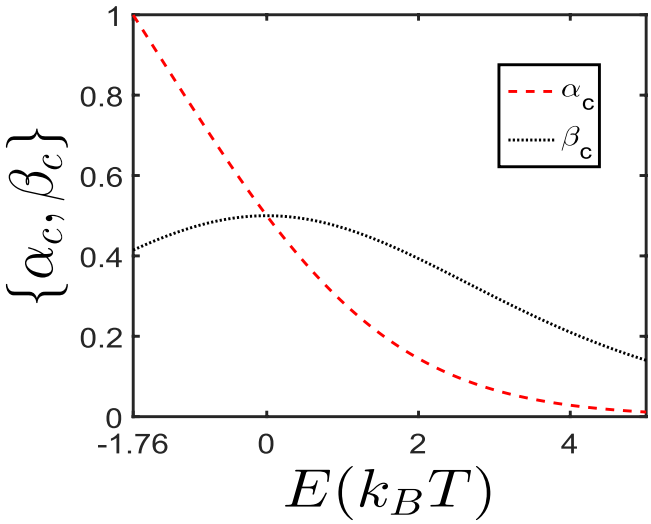

Figure 2. Triple points (α_c, β_c) as a function of interaction energy E for various values of θ, and for $\rho_{\rm MC} = 0.5$. The triple points remain invariant for any value of splitting parameter θ for $E > E_c(\theta = 1) \approx -1.76 k_{\rm B}T$ [21].

density becomes independent of E and is given as $\rho_{\rm MC} = 0.5$, and it yields the simplified expressions for triple points as $\alpha_c = \frac{2}{(1+q)^2}$, and $\beta_c = \frac{2q}{(1+q)^2}$. While for very strong repulsive interactions, i.e. for $E < -2.885 k_{\rm B}T$, $\rho_{\rm MC}$ does not remain constant and varies with E (refer [21]). The expression of triple points obtained using this $\rho_{\rm MC}$ are lengthy and thus makes the general theoretical calculations very complex for a network. Moreover, the experiments on motor proteins suggest the presence of weak interaction energy of range $E \approx 1.6 \pm 0.5 k_{\rm B}T$. Therefore, for producing the theoretical results for networks, we limit the range of interaction energy to $E > -2.885\ k_{\rm B}T$. Table 1 shows the bulk ($\rho_{\rm Phase}$), the left (ρ_1) and the right (ρ_L) boundary densities for the possible phases $\in$ {LD,HD,MC} of single channel interacting system for $E > -2.885 k_{\rm B}T$. Note that the particle-hole symmetry breaks at the boundary sites 1 and N. Thus the density at the first site for HD and MC phase is different from the bulk density and is obtained by equating the entrance current at first site, simplified under the simple mean-field arguments as $\alpha(1-\rho_1)[1+(q-1)\rho_{\rm phase}]$, with the bulk current in that phase. Similarly the particle density at the Nth site for LD and MC phase is different from the bulk density and is obtained by equating the simplified mean-field expression of exit current from site N, given by $\beta\rho_N[1+(r-1)\rho_{\rm Phase}]$ with the bulk current in that phase.

3. Network of many interacting TASEP segments

3.1. Description of network $V(m:n)$

We consider a network $V(m:n)$ of interacting TASEP segments. In the network $V(m:n)$, m similar interacting TASEP segments A_1, A_2, $\cdots$, A_m meet at a vertex (or junction site) v. From the vertex v, the n similar interacting segments B_1, B_2, $\cdots$, B_n diverges. The vertex v is assumed as a special site with density $\tilde{\rho}$ (see figure 3). Each TASEP segment consists of N sites and thus the complete network is considered as a

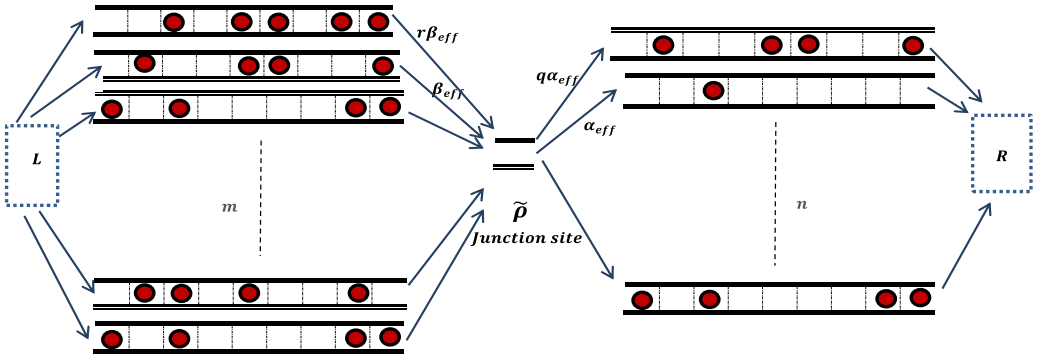

Figure 3. Schematic view of a vertex $V(m:n)$ with density $\tilde{\rho}$ and m incoming and n outgoing segments.

system with $(m+n)N+1$ sites. Each site can either be empty or occupied. We assign an occupation variable τ_i^j to each ith site of the jth lattice branch, where $i \in \{1, 2, \cdots L\}$ and $j \in \{1, 2, \cdots, m+n\}$ lattice. Let τ_v denotes the occupation variable for the vertex v. It is to be noted that in our model, the particles follow the random-sequential update rule and they are only allowed to move forward with no vertical lane changing.

The rate of entrance of a particle from the left reservoir 'L' into the first site of any of the left m incoming segments is α if the second site of the segment is empty; otherwise the entrance rate is $q\alpha$. A particle present at the last site of any of the left m segments exits into the junction site v with a rate $\beta_{\text{eff}} = (1-\tilde{\rho})$ if its left neighboring site is empty; otherwise the rate of leaving is $r\beta_{\text{eff}}$, due to the breakage of bond between the particles sitting at the last two sites of the segment. The junction site v is thus interpreted as a finite right reservoir for the left m segments.

The vertex v with density ρ_v also act as a finite left reservoir for the right segments B_1, B_2, ⋯, B_n from which the probability of entrance of a particle to any of the right segments is same. A particle can thus enter with an entrance rate $\alpha_{\text{eff}} = \frac{\tilde{\rho}}{n}$, if the segment's B_l, where $l \in \{1, 2, \cdots, n\}$, first as well as the second site is empty, whereas the rate is entrance is $q\alpha_{\text{eff}}$, when the segment's first site is empty but the second site is occupied. The particles at the last site of the segments $B_l s'$ exit to the right reservoir R with the same rates defined for the individual segments in section 2 (see figure 1). The explicit dependence of the exit and entrance rates of segments $A'_k s$ and $B'_l s$, respectively on the vertex density $\tilde{\rho}$ ensures the effective coupling between the left segments and the right segments.

In the absence of the junction site, the system is decoupled and all the lattice branches behave identically as a single-channel interacting TASEP model, whose properties have been well examined [21].

3.2. Explicit-vertex framework

We employ the explicit-vertex framework to determine the dynamics of the entire network [27]. In the approach, the vertex is introduced explicitly as an additional site. It couples the m parallel left incoming interacting TASEP segments with the decoupled n right outgoing interacting TASEP segments (as shown in section 3.1). To determine the overall state of the system, we examine the master equation for the vertex v in the

J. Stat. Mech. (2019) 083202

steady-state. The equation implies that the total particle current entering at vertex v is equal to the total particle current leaving from the vertex v. The particle current in each of the left m segments is a function of entrance rate α, interaction energy E and exit rate $\beta_{\text{eff}}(\tilde{\rho})$. We denote the particle current in any of the left segments $A_k's$ by $J_{A_k}(\alpha, \tilde{\rho}, E)$, where $k \in \{1, 2, \cdots m\}$. Since, the bulk as well as boundary dynamics of segments A_1, A_2, $\cdots$, A_m are same, we write $J_{A_1} = J_{A_2} = \cdots J_{A_m} = J_A(\alpha, \tilde{\rho}, E)$. Similarly, the particle current in segments B_1, B_2, $\cdots$, B_n is identical and is a function of $\tilde{\rho}$, β, and E. We denote the particle current in these segments by $J_{\text{B}}(\tilde{\rho}, \beta, E)$. The current continuity condition at vertex v gives

$$mJ_A(\alpha, \tilde{\rho}, E) = nJ_{\text{B}}(\tilde{\rho}, \beta, E). \tag{2}$$

The above condition can be utilized to obtain the vertex density $\tilde{\rho}$, and hence the effective exit and the effective entrance rates of left and right segments, respectively. Once, we have obtained the effective entrance rate, we can determine the properties of all the left m incoming segments to vertex v from its mapping to a single interactive TASEP segments with the entrance rate α and exit rate $\beta_{\text{eff}}(\tilde{\rho})$. Similarly, we can obtain the steady-state properties of the right n outgoing segments by mapping them to a single interactive TASEP segment with entrance rate $\alpha_{\text{eff}}(\tilde{\rho})$ and exit rate β. Thus, by using the well expressed cluster mean-field results of single channel interacting TASEP segment in terms of entrance and exit rates given in table 1 and section 2, we can determine all the dynamical properties of the entire network.

4. Stationary phase diagrams

We now explore the effect of interactions, the number of incoming and outgoing segments on the topology of the phase diagram of a network $V(m : n)$ consisting of $m + n$ interacting TASEP segments. In the proposed network $V(m : n)$, all the m incoming interacting TASEP segments ($A_k's$), where $k \in \{1, 2, \cdots m\}$, behave identically and thus for given parameters $\alpha, \tilde{\rho}$ and E, they exist in the same phase among the three possible phases (LD, HD, and MC) in a phase diagram. Similarly, all the n outgoing interacting TASEP segments ($B_l's$), where $l \in \{1, 2, \cdots n\}$, have identical dynamics and hence all of them together exist in one same phase among the LD, HD, and MC phases for the given parameters $\tilde{\rho}, \beta$ and E in a phase diagram. It is thus expected that the complete network can have nine possible phases. We use the notation $P_1 : P_2$ to label a phase in a network $V(m : n)$, where P_1 and P_2, respectively describe a phase in the left and the right side segments, while the colon separates the two phases.

Among the nine possible phases, the certain phases in a phase diagram can appear only for particular relation between the number of incoming segments m and the number of outgoing segments n. For instance, we observed that the MC:MC phase can exist only for $m = n$. To understand the reason for such existence, we first note that, in general, a phase $P_1 : P_2$ exists, if the equation $mJ_{P_1,A} = nJ_{P_2,B}$ can be solved for the unknown vertex density $\tilde{\rho}$, where $J_{P_1,A}$ represents the current in phase P_1 for segment A. Further, if, in addition, the solution $\tilde{\rho}$ also satisfy the simultaneous existence condition for the phases P_1 and P_2, given the values of α and β, then the

J. Stat. Mech. (2019) 083202

phase $P_1 : P_2$ exist, otherwise not. Now, in the MC:MC phase, the maximal current depends on the bulk dynamics and is independent of entry and exit rates. Since the bulk behavior of all the segments $A_k's$ and $B_l's$ are same, we obtain the same maximal current in all the segments for a given interaction energy E. Hence, the existence condition $mJ_{\mathrm{MC},A} = nJ_{\mathrm{MC},B}$, for the MC:MC phase, can hold only for $m = n$. Similarly, the phases HD:MC, LD:MC (MC:LD, MC:HD) can exist only for $m > n$ ($m < n$). This is because the particle current $J_{\mathrm{HD},A} < J_{\mathrm{MC},A}$ ($J_{\mathrm{LD},B} < J_{\mathrm{MC},B}$), therefore the condition $mJ_{\mathrm{HD},A} = nJ_{\mathrm{MC},B}$ ($mJ_{\mathrm{MC},A} = nJ_{\mathrm{LD},B}$), for the phase HD:MC (MC:LD) to exist, can be satisfied only for $m > n$ ($m < n$). We now derive the spanning regions and discuss the properties and existence conditions of all the possible phases.

(a) LD:LD: This is the phase when all the left m segments and all the right n segments are in LD phase. The LD phase in the incoming segments can exist when $\alpha < \alpha_c$ and $\alpha < \frac{\beta_{\mathrm{eff}}}{\sqrt{q/r}}$. Whereas the LD phase in the right n segments exists for $\alpha_{\mathrm{eff}} < \alpha_c$ and $\alpha_{\mathrm{eff}} < \frac{\beta}{\sqrt{q/r}}$. This implies that LD:LD phase can exist, if the possible solution $\tilde{\rho}$ of the equation $mJ_{\mathrm{LD},A} = nJ_{\mathrm{LD},B}$ satisfies the condition

$$0 < \tilde{\rho} < \min\left\{1 - \frac{\alpha}{\sqrt{r/q}}, \frac{n\beta}{\sqrt{q/r}}, n\alpha_c\right\}, \quad \alpha < \alpha_c. \tag{3}$$

In particular, for $\theta = 0.5$, $\alpha_c = \frac{2}{(1+q)^2}$, $\beta_c = \frac{2q}{(1+q)^2}$, and then LD:LD phase exists, if $\tilde{\rho}$ satisfies

$$0 < \tilde{\rho} < 1 - q\alpha, \quad \tilde{\rho} < n\beta/q, \quad \tilde{\rho} < 2n/(1+q)^2, \ \textit{and}\ \alpha < 2/(1+q)^2.$$

The above relations imply that LD:LD phase can exist for any number of incoming and outgoing segments and for any finite value of energy E. In particular, the relation $0 < \tilde{\rho} < 1 - q\alpha$ also implies that

$$\alpha < \frac{1}{q}. \tag{4}$$

Since for attractive energy $q > 1$ and for repulsive interaction energy $q < 1$, the above inequality indicate that with the increase in the attractive interaction energy, the LD:LD region shrinks, while the region gets enlarged for high repulsive interactions. This is physically justified because repulsive interactions pull particles away from each other, thus maximize the LD region, while the attractive interactions cause particles to make big clusters and hence the LD region is minimized in this case.

(b) HD:HD: In this phase, all the incoming and outgoing segments of the network are in the HD phase. The particle current in the incoming segments are dominated by the effective exit rate β_{eff} and exists when $\alpha > \frac{\beta_{\mathrm{eff}}}{\sqrt{q/r}}$ and $\beta_{\mathrm{eff}} < \beta_c$, while

J. Stat. Mech. (2019) 083202

the particle current in the outgoing segments is dominated by the exit rate β, and the existence condition for the phase is $\alpha_{\text{eff}} > \frac{\beta}{\sqrt{q/r}}$ and $\beta < \beta_c$. Therefore, the HD:HD phase subsists if the possible solution $\tilde{\rho}$ of the equation $mJ_{\text{HD},A} = nJ_{\text{HD},B}$, simultaneously satisfies the existence conditions for both the phases, which is simplified to

$$\tilde{\rho} > max\left\{1 - \frac{\alpha}{\sqrt{r/q}}, \frac{n\beta}{\sqrt{q/r}}, 1 - \beta_c\right\}, \quad \beta < \beta_c. \tag{5}$$

Since the probability of the filled vertex site can not be greater than 1, the above condition gives the following relation between the exit rate β, rate q, and total number of outgoing segments for $\theta = 0.5$:

$$\beta < \frac{q}{n}. \tag{6}$$

It implies that for a fixed n, the HD phase occupies more area for attractive interaction while the reverse happens for the case of repulsive interactions. This is also physically justified because of the nature of attractive interactions that favor large clusters of particles while the repulsive interactions pull the particles away from each other. We also conclude from equation (6) that for a fixed interaction energy, whether attractive, zero or repulsive, the HD region shrinks with the increase in the total number of outgoing segments. This is justified because with the increase in n, the rate of entrance of each of the right segments to v decreases, which favor the diminishing of the HD phase in these segments.

(c) HD:LD: When the left segments $A_k's$ are in HD phase while the right hand segments $B_l's$ are in LD phase, then we say the network $V(m:n)$ is in HD:LD phase. The existence conditions for the left segments and right segments from their mapping to a single interactive TASEP segments with the respective entrance-exit rates as α, β_{eff}, and α_{eff}, β yield the following three conditions for vertex density $\tilde{\rho}$.

$$1 - \beta_c < \tilde{\rho} < n\alpha_c, \qquad \text{for } \alpha \geqslant \alpha_c,\ \beta \geqslant \beta_c, \tag{7}$$

$$1 - \frac{\alpha}{\sqrt{r/q}} < \tilde{\rho} < \frac{n\beta}{\sqrt{q/r}},\ \tilde{\rho} < n\alpha_c, \quad \text{for } \alpha < \alpha_c, \tag{8}$$

$$1 - \frac{\alpha}{\sqrt{r/q}} < \tilde{\rho} < \frac{n\beta}{\sqrt{q/r}},\ \tilde{\rho} > 1 - \beta_c, \quad \text{for } \beta < \beta_c. \tag{9}$$

If the solution, $\tilde{\rho}$ for the equation $mJ_{\text{HD},A} = nJ_{\text{LD},B}$ satisfy either of the above three inequalities, then the phase HD:LD exists in that region. Moreover for $\theta = 0.5$, the above complex inequalities give the following simplified relation between energy E and number of segments n

J. Stat. Mech. (2019) 083202

$$q < \sqrt{2n-1}, \quad or \quad E < 2\ln(\sqrt{2n-1}). \tag{10}$$

Equation (10) gives the upper bound on the energy E or rate q for the existence of the HD:LD phase depending on n. For the case of $n = 1$, the equation (10) disapproves the existence of HD:LD phase for attractive and zero interactions for any value of m. This can be verified for the particular case of $m = 2$ given in [26], where the HD:LD phase did not exist for $E = 0$. Now, when $n = 2$, equation (10) implies that the HD:LD phase can exist only if $q < \sqrt{3}$. This is also verified with the known result for the particular case of $m = 2$ in [27], where the HD:LD phase existed for $q = 1 < \sqrt{3}$.

(d) MC:MC: This phase is independent of the entrance rate α and exit rate β. It exists for $\alpha \geqslant \alpha_c$, $\beta \geqslant \beta_c$ provided $m = n$ and α_c, β_c satisfy the following relation.

$$n\alpha_c \leqslant 1 - \beta_c. \tag{11}$$

In particular, for $\theta = 0.5$, we get that MC:MC phase exists only when

$$q \geqslant \sqrt{2n-1}, \quad or \quad E \geqslant 2\ln(\sqrt{2n-1}). \tag{12}$$

We observe that for the case of $m = n$, the existence conditions for the phase HD:LD and phase MC:MC, given, respectively by equations (10) and (12) are complimentary to each other. This implies that the two phases can not exist simultaneously in a phase diagram. Figure 4(a) shows the critical interaction energy curve depending on n, above which the MC:MC phase occurs, while in the compliment area the HD:LD phase is found. Remarkably, figure 4(a) implies that the MC:MC phase can never exist for repulsive energy. The consequence of this interesting finding in the framework of biological molecular motors will be discussed in section 5. Also, when $m = n = 2$, the MC:MC phase can occur only for $q \geqslant \sqrt{3}$ or $E \geqslant E_{c_1}$, which is true as MC:MC does not exist even for $E = 0$ [27]. While we observe from figure 5(d) that for the case of attractive interactions, $E = 1.6k_BT$, the HD:LD phase is replaced by the MC:MC phase.

(e) HD:MC: This phase occurs only when $m > n$ and when the solution $\tilde{\rho}$ of the equation: $mJ_{\mathrm{HD},A} = nJ_{\mathrm{MC},B}$, satisfies the condition

$$\tilde{\rho} > max\{1 - \beta_c, n\alpha_c\}. \tag{13}$$

In particular for the critical values for $\theta = 0.5$, the condition 13 is possible for

$$q > \sqrt{2n} - 1, \ or \ E > 2\ln(\sqrt{2n} - 1). \tag{14}$$

Equation (14) implies that, for $m > n$, the HD:MC phase occurs for $E > 2\ln(\sqrt{2n} - 1)$, as shown by the fully filled region above the blue curve in figure 4(b). While equation (10) implies that the HD:LD phase is possible for $E < 2\ln(\sqrt{2n-1})$, the region filled with the vertical lines under the red curve in figure 4(b). This

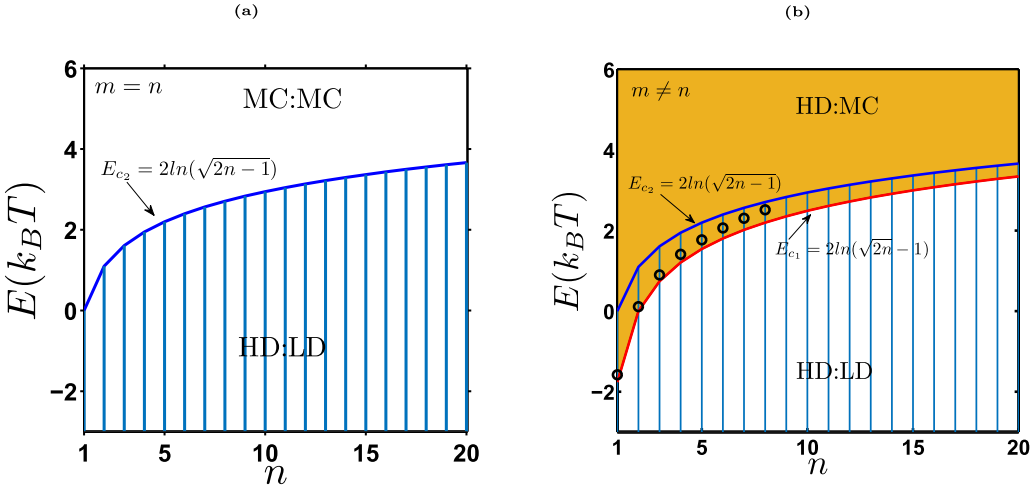

Figure 4. (a) Plot of critical interaction energies separating the existence of HD:LD (shaded region with vertical lines) and MC:MC phases for $m = n$, as function of n. (b) Blue (red) curve represents the upper (lower) bound, given as $E_{c_2}(E_{c_1})$ for the critical interaction energy with respect to n below (above) which HD:LD (HD:MC) phase can exist. The plot of critical interaction energies separating the two phases for $m > n$, which depends on m and n is marked by circles in the common region, for a fixed $m = 10$ and as function of n.

implies that for the energies between $2\ln(\sqrt{2n}-1) < E < 2\ln(\sqrt{2n-1})$, there is a possibility of the occurrence of both the HD:LD and HD:MC phases (see the region which is shaded and as well as has vertical lines in figure 4(b)). However, for given values of m, n and E, with $m > n$, only one of the phase can exist depending on whether the solution $\tilde{\rho}$ for the equation $mJ_{\mathrm{HD},A} = nJ_{\mathrm{LD},B}$ satisfy either of the inequalities given by equations (7)–(9) or the solution $\tilde{\rho}$ of the equation: $mJ_{\mathrm{HD},A} = nJ_{\mathrm{MC},B}$, satisfies the equation (13). To determine the phase within the intersection of two regions, which depends on m, we numerically solve the corresponding current equations for $\tilde{\rho}$ for a fixed $m = 10$ and n varying from 1 to 8 and found the critical interacting energies for the existence of the two phases (see the black filled circles in inset of figure 4(b)). We observed that for $m \gg n$, the bottom solid line represented by the curve: $E_{c_1} = 2\ln(\sqrt{2n}-1)$, separates the existence of the two phases. While as $m - n \to 1$, the red upper curve, given by $E_{c_2} = 2\ln(\sqrt{2n-1})$ yields the critical energies for the existence of the two phases. We verify these results for the case of $m = 2$ and $n = 1$. Equation (14) implies that the HD:MC phase occurs if $\tilde{\rho}$ satisfies $mJ_{\mathrm{HD},A} = nJ_{\mathrm{MC},B}$ for $q > \sqrt{2}-1$ or $E > -1.7627$. This is true as seen for $E = 0$ that HD:MC phase exists [26].

(f) MC:LD: This phase can only occur if $m < n$ and the solution $\tilde{\rho}$ of equation: $mJ_{\mathrm{MC},A} = nJ_{\mathrm{LD},B}$, satisfies the condition

$$\tilde{\rho} < \min\left\{1 - \beta_c, n\alpha_c\right\}. \tag{15}$$

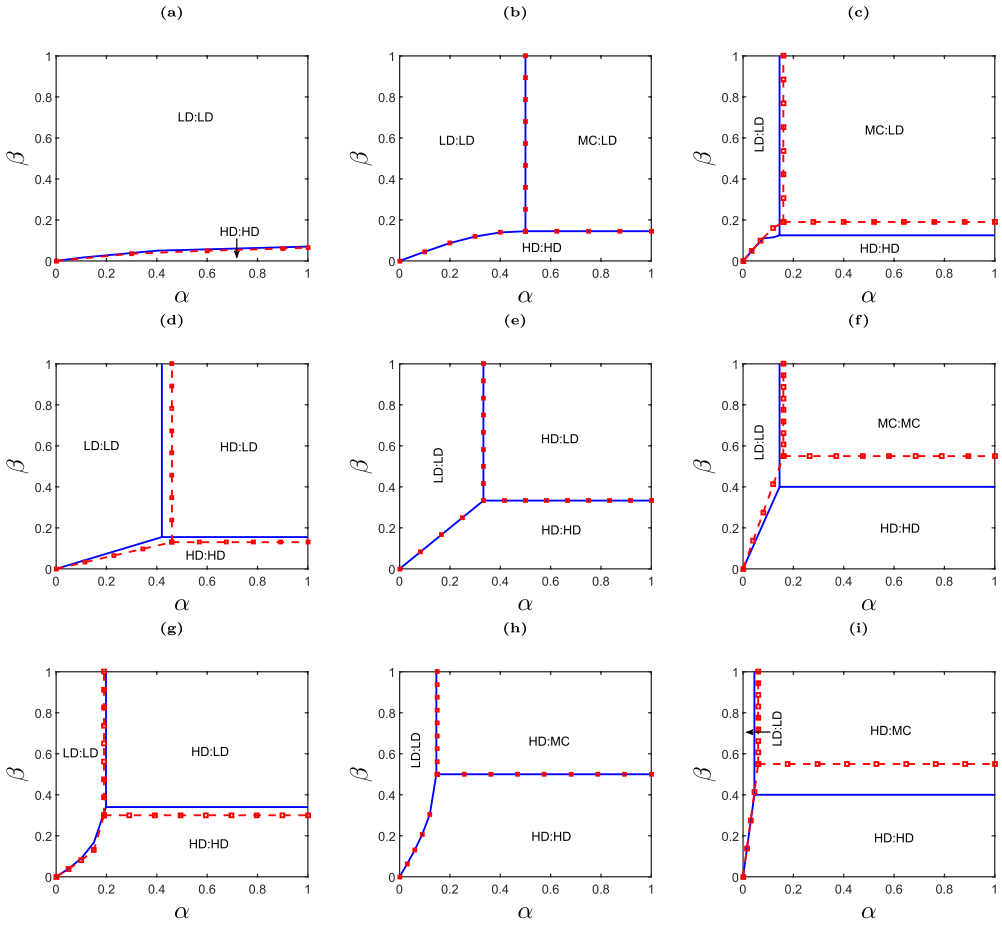

Figure 5. Stationary phase diagrams for ((a)–(c), i.e. row 1) $m = 1$ and $n = 2$; ((d)–(f), i.e. row 2) $m = 2$ and $n = 2$; ((g)–(i), i.e. row 3) $m = 2$ and $n = 1$ and for interaction energies $E = -2\ k_{\rm B}T$ in column 1 (i.e. (a), (d), (g)); $E = 0\ k_{\rm B}T$ in column 2 (i.e. (b), (e), (h)) and $E = 2\ k_{\rm B}T$ in column 3 (i.e. (c), (f), (i)). Solid blue lines correspond to theoretical results and dotted red lines with symbols represent the Monte Carlo simulation results for each segment having $N = 500$ sites.

In particular, for $\theta = 0.5$, this phase can exist for any value of E provided the solution $\tilde{\rho} < \min\left\{\frac{q^2+1}{(1+q)^2}, \frac{2n}{(1+q)^2}\right\}$.

For the remaining three possible phases LD:MC, LD:HD, and MC:HD, we noticed that the particle current in the LD and the MC phases for segments $A'_k s$ and in the HD and the MC phases for segments $B'_l s$ is independent of the vertex density ($\tilde{\rho}$). Thus, the current equality conditions for the corresponding phases, LD:HD, LD:MC, and MC:HD, in a network can either yield a phase transition curve or a line but can not span a region in the (α, β) parameter space. For instance, the condition $mJ_{{\rm LD},A} = nJ_{{\rm MC},B}$ for the phase LD:MC can only yield a phase transition line: $\phi_1(m, n, E, \alpha) = 0$. On the same arguments, we can say that the condition $mJ_{{\rm MC},A} = nJ_{{\rm HD},B}$ for the existence of the phase MC:HD yields a phase transition line $\phi_2(m, n, E, \beta) = 0$. Similarly, the current matching condition: $mJ_{{\rm LD},A} = nJ_{{\rm HD},B}$ for the phase LD:HD, produces a phase transition curve or a line with a finite and non-zero slope in the (α, β) parameter space.

J. Stat. Mech. (2019) 083202

Thus, there can exist only six regions, namely, LD:LD, HD:LD, HD:HD, HD:MC, MC:LD and MC:MC in a phase-diagram of a network $V(m:n)$.

5. Results and discussions

In the previous section, we theoretically computed the general existence conditions for the possible phases in a phase diagram for a network with '$m+n$' interacting TASEP segments meeting at a vertex v. In order to validate our general approximate theoretical results, we perform extensive computer Monte Carlo simulations for some fixed particular values of m and n. Moreover, we also observed from figure 4 that the phases do not further change for higher interaction energy and large number of outgoing segments. Therefore, we perform simulations for the weak and moderate interaction energy, which is also relevant to biological molecular motors. Further, to observe the effect of interaction energy on the network and to compare our results with the known results for zero energy, we consider the fix values $m=n=2$ [27] for the case when the number of incoming and outgoing segments are equal. But, when number of incoming segments and outgoing segments are unequal, we choose the fix values $m=2, n=1$ for $m>n$ and $m=1$ and $n=2$ for $m<n$, for comparing our results with the results in [26].

Figure 5 shows the stationary phase diagram for repulsive (column 1), zero (column 2) and attractive energy (column 3) for different values of m and n. We have re-plot the phase diagrams for zero energy for comparing the results of interaction energy. Our theoretical findings are in agreement with the Monte Carlo simulations. We find that the interactions in a network of several TASEP segments not only shift the boundaries but also has non trivial effect on the topology of the phase diagrams. For the case when $m<n$, i.e. $m=1, n=2$ (see figures 5(a)–(c)), we find that with the increase in the repulsive energy, the MC:LD phase diminishes, while the LD:LD region expands, and the HD:HD region shrinks. On the contrary, the attractive interactions shrink the LD:LD phase, but expand the MC:LD and HD:HD regions. For $m=n=2$, we find that the HD:LD phase that exists for $E=0$ vanishes for $E>1.1\ k_{\mathrm{B}}T$ and instead get replaced by the MC:MC phase (see figures 5(e) and (f)), where the critical energy $E\approx 1.1\ k_{\mathrm{B}}T$ is obtained for $n=2$ from the theoretical relation $E_{c_2}=2\ln(\sqrt{2n-1})$ that determines the existence of HD:LD region. The attractive energy due to more particle cluster formation also shrinks the LD:LD phase and enlarges the HD:HD phase: see figure 5(f). While for the repulsive interactions, the region for LD:LD phase enlarges and the HD:HD region shrinks due to the separation among the particles in this scenario. Figures 5(g)–(i) shows the phase diagrams for $m=2$, $n=1$ for $E=-2.0\ k_{\mathrm{B}}T$, $E=0.0\ k_{\mathrm{B}}T$, and $E=2.0\ k_{\mathrm{B}}T$, respectively. It was observed that as the interaction energy decreases from positive to negative, the LD:LD region expands, while the HD:HD phase shrinks. This is in accordance with the results shown by equations (4) and (6), which shows the direct dependence of the HD region on energy E, while the LD region was inversely proportional to E. We also observe that for a given pair of m and n, the topology of the phase diagram changes with an appearance of HD:MC phase and continuous disappearance of HD:LD phase after a critical interaction strength

J. Stat. Mech. (2019) 083202

$E_{c_1} > 2\ln(\sqrt{2n}-1)$ for $m \gg n$. While the critical interaction strength for the phase change between HD:MC and HD:LD for $m-n \to 1$ is given as $E_{c_2} = 2\ln(\sqrt{2n-1})$. This is evident from figures 5(a) and (b), where the HD:MC phase existed for attractive energy $E = 1.6k_BT$ (figure 5(a)) and weak repulsive $E = -1k_BT$ (figure 5(b)), but the phase changes to the HD:LD phase for higher repulsive energy $E = -1.6k_BT$ (figure 5(c)). This is also physically justified since the repulsive interactions favor the LD phase due to the repulsions between the particles.

Experiments on motor proteins suggest the presence of attractive interactions within the range $E \approx -1.6 \pm 0.5\ k_BT$ among the molecular motors [24]. It is interesting to observe whether such range of energy optimize the flow of molecules or not. The recent study of single channel thermodynamically consistent interacting TASEP model indicated that the weak repulsive energy is required for the maximal flow of particles [20]. However, the model was single channel and the realistic work environment of motor proteins involves complex microtubule network, the observation for the single channel model can not be generalized. In the proposed network, we find that for the special case when number of incoming segments is equal to the number of outgoing segments, i.e. $m = n$, there exists the interaction energy depending on n given by $E_{c_3} = 2\ln(\sqrt{2n-1})$ beyond which the MC:MC phase exist in the complete network. The critical interaction energy implies that for any value of n that the motor proteins can not optimize their transport for the repulsive energy. Moreover, it suggests that for current to maximize in a network, they must operate under the attractive energy, as observed in the experiments. The above finding is evident from figure 5(f), which shows the phase diagram for $m = n = 2$ and $E = 2.0k_BT$. In comparison to the case of zero energy where the MC:MC phase can not exist for $n = 2$ (see figure 5(e)), we found using the existence condition that the MC:MC phase exists for all attractive energy greater than $E \approx 1.1k_BT$.

The vehicular transport in a highway network of converging and diverging roads often deals with the presence of repulsive interactions among the vehicles, it is found that when there is only one outgoing segments and the number of incoming segments is more than one. Then, even in the presence of repulsive interactions, the outgoing segment can have the maximal current phase, while in the incoming segments being greater than one can not be found in the MC phase. If the number of outgoing segments are more than one, then they can be found in the MC phase only in the presence of attractive interactions. We also plot the density profiles for the different phases in figure 6. There is an excellent agreement between the theoretical and simulation results.

5.1. Correlations

The correlations have played an important role in determining the dynamical properties of the system for a single channel interacting TASEP model, Basically, a two-point correlation function for a single lattice gives a measure of how the presence of the particle sitting at site i affects the occupation of the neighboring site $i+1$. The results for the single channel interacting TASEP system suggested that the correlations are weaker, negative and *short-range* for the repulsive interactions, while they are stronger, positive and *long range* for the attractive interactions [25]. It was also concluded that two-cluster mean-field analysis for the model was sufficient to handle the weak

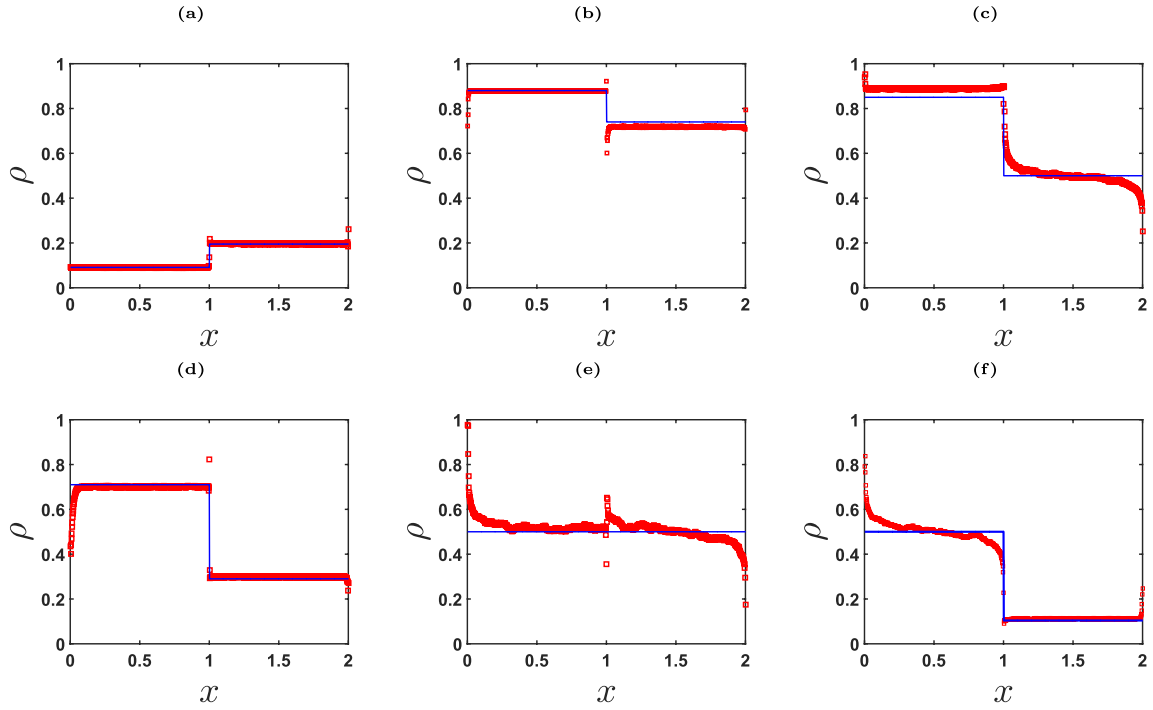

Figure 6. Density profiles for different stationary phases with $m = 2$. (a) LD:LD phase for $n = 1$, $E = -1.6\ k_{\mathrm{B}}T$, $\alpha = 0.1$, $\beta = 0.6$; (b) HD:HD phase for $n = 1$, $E = -1\ k_{\mathrm{B}}T$, $\alpha = 0.6$, $\beta = 0.2$; (c) HD:MC phase for $n = 1$, $E = -1\ k_{\mathrm{B}}T$, $\alpha = 0.6$, $\beta = 0.8$; (d) HD:LD phase for $n = 2$, $E = -1.6\ k_{\mathrm{B}}T$, $\alpha = 0.6$, $\beta = 0.8$; (e) MC:MC phase for $n = 1$, $E = 1.6k_{\mathrm{B}}T$, $\alpha = 0.6$, $\beta = 0.8$; (f) MC:LD phase for $m = 1$, $n = 2$, $E = 1.6k_{\mathrm{B}}T$, $\alpha = 0.4$, $\beta = 0.4$. Here $x = i/N$, where $i \in \{1, 2, \cdots, N\}$ represents the lattice sites for a left incoming segment and i varying from $N + 1$ to $2N$ represents the lattice sites for the right outgoing segments. Solid blue lines correspond to theoretical results and red symbols represent the Monte Carlo simulation results for each segment having $N = 500$ sites.

correlations but for a more elaborate analysis of the single channel system with strong interactions, one require a further advanced theory.

Here, we aim at focusing on how a two-point correlation function affect the dynamics of a complex network consisting of many interacting TASEP system and also we find whether the two-cluster mean-field theory is strong enough to handle correlations in this large network of interacting TASEP system. For this, we compute the two-point nearest-neighbor correlations in the segments left to the vertex v as well as in the segments right to the vertex v. Since the dynamics of all the left segments is same and also the dynamics of all the right segments is identical, we compute a general two-point correlation function in one of the left segment (say) A as well as in one of the right segment (say) B, defined as

$$C_i = \langle \tau_i \tau_{i+1} \rangle - \langle \tau_i \rangle \langle \tau_{i+1} \rangle = P(\tau_i = 1, \tau_{i+1} = 1) - P(\tau_i = 1) P(\tau_{i+1} = 1) = P_{11} - \rho^2, \tag{16}$$

where τ_i, $\langle \cdots \rangle$ denotes the occupancy state of any site i and the statistical average, respectively and P_{11} denotes the probability of the two-cluster (1,1). Note that we have

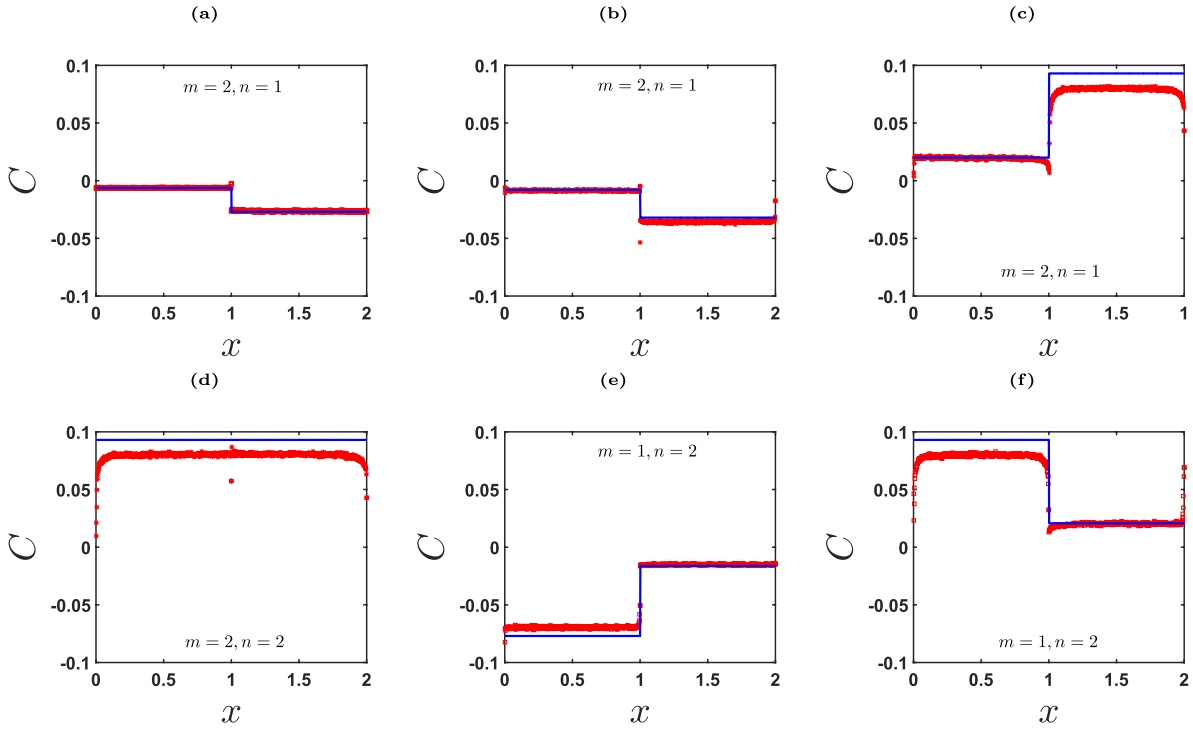

Figure 7. Correlation profiles in different stationary phases for stated values of m, n and (a) LD:LD phase for $E = -1.6\ k_{\mathrm{B}}T$, $\alpha = 0.1$, $\beta = 0.6$; (b) HD:HD phase for $E = -1\ k_{\mathrm{B}}T$, $\alpha = 0.6$, $\beta = 0.2$; (c) HD:MC phase for $E = 1.6\ k_{\mathrm{B}}T$, $\alpha = 0.6$, $\beta = 0.8$; (d) MC:MC phase for $E = 1.6 k_{\mathrm{B}}T$, $\alpha = 0.6$, $\beta = 0.8$; (e) LD:LD phase for $E = -1.6\ k_{\mathrm{B}}T$, $\alpha = 0.6$, $\beta = 0.8$; (f) MC:LD phase for $E = -1.6\ k_{\mathrm{B}}T$, $\alpha = 0.6$ and $\beta = 0.8$. Here $x = i/N$, where $i \in \{1, 2, \cdots, N\}$ represents the lattice sites for a left incoming segment and i varying from $N+1$ to $2N$ represents the lattice sites for the right outgoing segments. Solid blue lines correspond to theoretical results and red symbols represent the Monte Carlo simulation results for each segment having $N = 500$ sites.

only considered correlations within each segment and have ignored the correlations between the boundary sites of the segments connecting through the vertex.

Figure 7 shows the correlation profiles for varying interaction energy and different values of m and n. We first investigate the effect of m and n on the strength of the correlations. It is clear from the figure that for $m > n$, the magnitude of correlations are larger at the exiting segments (see figures 7(a)–(c)). While for the case of $m < n$, the correlations becomes higher in magnitude at the incoming segments: see figures 7(e) and (f). These observations can be explained as follows. When $m < n$, the incoming total flux from the m left segments to the n outgoing segments gets diluted and as a result correlations becomes weaker in the exiting segments. Similarly, when $m > n$, the particle current gets more concentrated at the outgoing segments which makes the correlations stronger in them. But when $m = n$, the correlations in entering as well as exiting segments are equal (see figure 7(d)) as the particle flux in all the segments is same. We now observe the effect of interaction energy on the correlations. The correlations are found to be negative for $E < 0$: see figures 7(a), (b) and (e). This implies that the probability to find a particle at a site next to a given occupied site is less due to being

J. Stat. Mech. (2019) 083202

energetically unfavorable. For the attractive interactions, figures 7(c), (d) and (f), the correlations are positive as here the probability for finding the particle at the neighboring site is higher. Moreover, figure 7 also indicate that the two cluster mean-field theory sufficiently captures the correlations in the proposed system.

6. Conclusion

To summarize, we have considered a complex topology of interacting TASEP segments. In particular, we have explored a network $V(m:n)$, which consists of m incoming segments to a junction site v and n outgoing segments from the vertex v. The junction site is viewed as a reservoir of finite density, from where several segments converge and diverge. Correlations within the segments are treated in a cluster mean-field sense, while at the junction site, we ignore the correlations and employ the simple mean field approximation. We theoretically obtain the critical conditions for the existence of all the possible phases in the system. We found that among the nine possible phases, a phase diagram consists of only three phases at a time depending on E, m and n. We validated our theoretical results for fixed values of m and n with the computer Monte Carlo simulations. Our theoretical findings are generalized in terms of m, n and reproduce the results for the case of zero interactions. We observed that when the number of incoming and outgoing segments are equal, the maximal current phase in all the segments can exist only beyond some positive critical interaction energy. However, when $n = 1$ and $m > n$, the MC phase in the outgoing segments diminishes after some critical repulsive interaction strength. We also plot the phase diagrams, density, and the correlation profiles for various interaction strength, and number of incoming, outgoing segments. We found that the correlations in a network, $V(m:n)$, weakens among the segments which are large in number, due to the dilution of the particle flux. We also observed that with the increase in the total number of outgoing segments the probability of the HD phase decreases among them.

Acknowledgment

T Midha acknowledges DST, Govt. of India and IUSSTF for providing the Indo-US fellowship for women in STEMM, 2018. ABK acknowledges the support from the Welch Foundation (Grant C-1559), from the NSF (Grant CHE-1664218), and the Center for Theoretical Biological Physics sponsored by the NSF (Grant PHY-1427654).

References

[1] Chou T, Mallick K and Zia R 2011 *Rep. Prog. Phys.* **74** 116601
[2] Chowdhury D, Santen L and Schadschneider A 2000 *Phys. Rep.* **329** 199–329
[3] Domb C 2000 *Phase Transitions and Critical Phenomena* vol 19 (Amsterdam: Elsevier)
[4] MacDonald C T, Gibbs J H and Pipkin A C 1968 *Biopolymers* **6** 1–25
[5] MacDonald C T and Gibbs J H 1969 *Biopolymers* **7** 707–25
[6] Derrida B, Domany E and Mukamel D 1992 *J. Stat. Phys.* **69** 667–87
[7] Derrida B, Evans M R, Hakim V and Pasquier V 1993 *J. Phys. A: Math. Gen.* **26** 1493–517

J. Stat. Mech. (2019) 083202

[8] Krug J 1991 *Phys. Rev. Lett.* **67** 1882
[9] Schütz G and Domany E 1993 *J. Stat. Phys.* **72** 277–96
[10] Schadschneider A, Chowdhury D and Nishinari K 2010 *Stochastic Transport in Complex Systems: from Molecules to Vehicles* (Amsterdam: Elsevier)
[11] Antal T and Schütz G 2000 *Phys. Rev.* E **62** 83
[12] Chowdhury D 2013 *Phys. Rep.* **529** 1–197
[13] Kolomeisky A B and Fisher M E 2007 *Annu. Rev. Phys. Chem.* **58** 675–95
[14] Kolomeisky A B 2013 *J. Phys.: Condens. Matter* **25** 463101
[15] Midha T, Gomes L V, Kolomeisky A B and Gupta A K 2018 *J. Stat. Mech.* 053209
[16] Midha T, Kolomeisky A B and Gupta A K 2018 *Phys. Rev.* E **98** 042119
[17] Dierl M, Maass P and Einax M 2012 *Phys. Rev. Lett.* **108** 060603
[18] Dierl M, Einax M and Maass P 2013 *Phys. Rev.* E **87** 062126
[19] Pinkoviezky I and Gov N S 2013 *New J. Phys.* **15** 025009
[20] Teimouri H, Kolomeisky A B and Mehrabiani K 2015 *J. Phys. A: Math. Theor.* **48** 065001
[21] Midha T, Kolomeisky A B and Gupta A K 2018 *J. Stat. Mech.* 043205
[22] Katz S, Lebowitz J L and Spohn H 1984 *J. Stat. Phys.* **34** 497–537
[23] Vilfan A, Frey E, Schwabl F, Thormählen M, Song Y H and Mandelkow E 2001 *J. Mol. Biol.* **312** 1011–26
[24] Roos W H, Campàs O, Montel F, Woehlke G, Spatz J P, Bassereau P and Cappello G 2008 *Phys. Biol.* **5** 046004
[25] Celis-Garza D, Teimouri H and Kolomeisky A B 2015 *J. Stat. Mech.* P04013
[26] Pronina E and Kolomeisky A B 2005 *J. Stat. Mech.* P07010
[27] Embley B, Parmeggiani A and Kern N 2009 *Phys. Rev.* E **80** 041128
[28] Raguin A, Parmeggiani A and Kern N 2013 *Phys. Rev.* E **88** 042104
[29] Wang R, Liu M and Jiang R 2008 *Phys. Rev.* E **77** 051108
[30] Song X, Jiu-Ju C, Rui-Li W, Ming-Zhe L and Fei L 2009 *Chin. Phys.* B **18** 5103
[31] Wang X, Jiang R, Hu M B, Nishinari K and Wu Q S 2009 *Int. J. Mod. Phys.* C **20** 1999–2012
[32] Neri I, Kern N and Parmeggiani A 2011 *Phy. Rev. Lett.* **107** 068702
[33] Neri I, Kern N and Parmeggiani A 2013 *Phys. Rev. Lett.* **110** 098102
[34] Neri I, Kern N and Parmeggiani A 2013 *New J. Phys.* **15** 085005
[35] Denisov D V, Miedema D M, Nienhuis B and Schall P 2015 *Phys. Rev.* E **92** 052714

J. Stat. Mech. (2019) 083202